RSC Advances

PAPER

View Article Online
View Journal | View Issue

Cite this: *RSC Adv.*, 2020, **10**, 37555

Oligo-glycerol based non-ionic amphiphilic nanocarriers for lipase mediated controlled drug release†

Parmanand,[a] Ayushi Mittal,[a] Abhishek K. Singh,[ab] Aarti,[a] Katharina Achazi,[c] Chuanxiong Nie,[b] Rainer Haag[b] and Sunil K. Sharma *[a]

Received 28th August 2020
Accepted 3rd October 2020

DOI: 10.1039/d0ra07392j

rsc.li/rsc-advances

A new class of non-ionic amphiphiles is synthesized using a diaryl derivative of diglycerol as a central core and functionalizing it with long alkyl chains (C-12/C-15) and monomethoxy PEG moiety (M_n: 350/550) by following a chemo-enzymatic approach. The aggregation behavior of the amphiphiles in aqueous medium is studied by using dynamic light scattering (DLS) and fluorescence spectroscopy, whereas the size and morphology of the aggregates are studied by transmission electron microscopy (TEM). A hydrophobic dye, Nile red and a hydrophobic drug, nimodipine, are used to demonstrate the nano-carrier capability of these non-ionic amphiphilic systems and the results are compared with amphiphilic analogues obtained from the triaryl derivatives of triglycerol. The *in vitro* controlled release of the encapsulated dye is successfully carried out in the presence of immobilized *Candida antarctica* lipase (Novozym 435). Furthermore, cytotoxicity data is also collected which suggests that the amphiphiles are suitable for biomedical applications.

1. Introduction

The observance of self-assembly phenomena in lipids, carbohydrates, proteins and nucleic acids producing structurally precise and functional supramolecular architectures[1–6] has inspired researchers for the fabrication of structurally different and functional nano-structured materials having applications in various fields such as biomedicine and bio-technology.[7–11] Amongst the various promising applications of nano-architectures, drug delivery is of immense importance due to the concerns of lipophilicity and limited aqueous solubility associated with the commonly used drugs of low molecular weight (under 500 g mol^{-1}). Also, such drugs are known to diffuse rapidly in the body, have shorter circulation time, lack selectivity, and can interact through multiple binding sites leading to unwanted side effects.[12,13] Attempts have been made to address these issues by developing amphiphilic nano-structured drug delivery agents.[12,14–17] There are various traditional drug carriers *e.g.* PAMAM dendrimers, pluronics, liposomes, poly(lactic acid) (PLA) and poly(lactic-*co*-glycolic acid) (PLGA), *etc.* each having their own limitations. The pluronics have a fast degradation rate *in vivo* whereas in PAMAM, the probability of retro-Michael addition may restraint their shelf-life at the ambient conditions, lipoplexes favour non-specific electrostatic interactions with negatively charged hydrophobic serum albuminate, cellular components and other negatively charged systemic molecules and PLA/PLGA based nanocarriers exhibits burst release and poor loading of the drug.[13,18–20] In order to overcome these problems small non-ionic amphiphilic systems can enhance the properties of pharmaceutics in terms of solubility, bioavailability, and increase the lifetime of drug and selective release at the target site. Furthermore, the triggered release of drug in the body is an important aspect which is somehow missing in traditional drug delivery systems. Herein, stimuli responsive amphiphilic architectures have been explored for drug delivery and release. The reported nanocarriers possess ester linkages and their hydrolysis is lipase responsive facilitating the release of the drug. Such amphiphilic architectures facilitate a higher concentration of a drug to reach the target cell than would occur in the natural aqueous milieu and thus lowering the required dosage of the drug.

The amphiphilic nanocarriers can either be ionic or non-ionic, however, toxicity issues associated with ionic counterpart and particular with the cationic amphiphilic systems are widely reported, it makes them less important for biomedical applications. Cationic amphiphiles are known to exhibit non-specific electrostatic interactions with negatively charged hydrophobic serum albuminate, cellular components and other negatively charged systemic molecules. Due to such non-

[a]*Department of Chemistry, University of Delhi, Delhi 110 007, India. E-mail: sk.sharma90@gmail.com; Tel: +91-11-27666696*

[b]*Institut für Chemie und Biochemie, Freie Universität Berlin, Takustraße 3, 14195 Berlin, Germany*

[c]*Institut für Chemie und Biochemie, Freie Universität Berlin, Arnimallee 22, 14195 Berlin, Germany*

† Electronic supplementary information (ESI) available. See DOI: 10.1039/d0ra07392j

specific interactions, the transfection complexes bind to the biological cell surfaces and other systemic molecules, eventually leading to compromised with targeted lipofection. To address these issues, non-ionic amphiphilic architectures were introduced as an alternative to cationic ones. They offer many advantages over ionic amphiphilic architectures including better stability, pH independence, long shelf-life and minimum unwanted interaction, due to which non-ionic amphiphiles have preferred acceptance in the biomedical field.[13,21–23] Furthermore, most of the amphiphiles reported in literature for this purpose are either polymer or dendritic architectures produced from monomer moieties, however, replacing monomers with oligomers for the polymers synthesis is emerging as an interesting line of development.

Herein, our major focus is to design and develop newer amphiphilic architectures using oligomeric building blocks to have improved nanocarrier characteristics. The use of monomers leads to the formation of low molecular weight reaction products, which adversely affects the properties of the macromolecular compounds.[24,25] In contrast, glycerol oligomers may be used as superior building blocks for the synthesis of supramolecular architectures in polycondensation or polymerization reactions. The oligomers of glycerol such as di-, tri- and tetraglycerol have been well studied for various applications such as emulsifier, thickeners, and antifogging agents, *etc.*[26,27] Our group has earlier synthesized functionalized glycerol oligomers using a chemoenzymatic pathway.[27] As an extension of our ongoing research program to design and develop glycerol oligomers based nanocarriers, we decided to use diglycerol for the synthesis of amphiphilic nano-transporters as glycerol is renewable, nontoxic, and biodegradable.[28] Furthermore, as the hydrophilic–lipophilic balance (HLB) have a vital role in the aggregation and transport capacity of amphiphiles,[29,30] our interest is to fine tune the physicochemical characterization of amphiphilic systems by varying hydrophilic and hydrophobic components. For this purpose, monomethoxy-polyethyleneglycol (mPEG) is used because of its favorable properties such as aqueous solubility, non-toxicity, good chemical stability and biocompatibility.

We have synthesized a series of new non-ionic diglycerol-based amphiphilic compounds (**15–18**) that self-assemble in aqueous medium forming an inner hydrophobic core capable of encapsulating hydrophobic guest and its subsequent release under hydrolytic conditions (Fig. 1). For the construction of these amphiphiles two hydrophobic aliphatic acid moieties were attached *via* the primary hydroxyl groups of diglycerol, whereas hydrophilic (mPEG acid) moieties were attached to the secondary hydroxyl groups through an aromatic spacer, *i.e.*, *p*-hydroxybenzoic acid (Scheme 1). The self-assembly behavior of these amphiphiles was studied using fluorescence spectroscopy, DLS and TEM. Nile red and nimodipine were used as model hydrophobic guests to study the nanocarrier potential of amphiphiles.

2. Experimental section

2.1. NMR, IR, mass and GPC analysis

^{1}H and ^{13}C NMR spectrum were recorded on JEOL 400 and 100.5 MHz spectrometer, respectively; the solvent residual peak was used for referencing. The chemical shift values are on δ scale and coupling constant (J) values are in hertz. The IR spectra of the samples were recorded using either Perkin-Elmer FT-IR model 9 or Compact FT-IR Spectrometer ALPHA II from Bruker. Mass and GPC data were recorded on an Agilent-6530 Q-TOF LCMS and Waters GPC system equipped with a Waters 515 HPLC pump, respectively.

3. Results and discussion

A series of new non-ionic amphiphilic architectures have been synthesized by first preparing diaryloxydiglycerol core by the reaction of diacetoxydiglycerol (**3**) with methyl *p*-hydroxybenzoate by following Mitsunobu reaction to yield compound **4**. The compound **4** was subsequently hydrolyzed in two steps to give diaryloxydiglycerol **6**. It was reacted further with propargyl

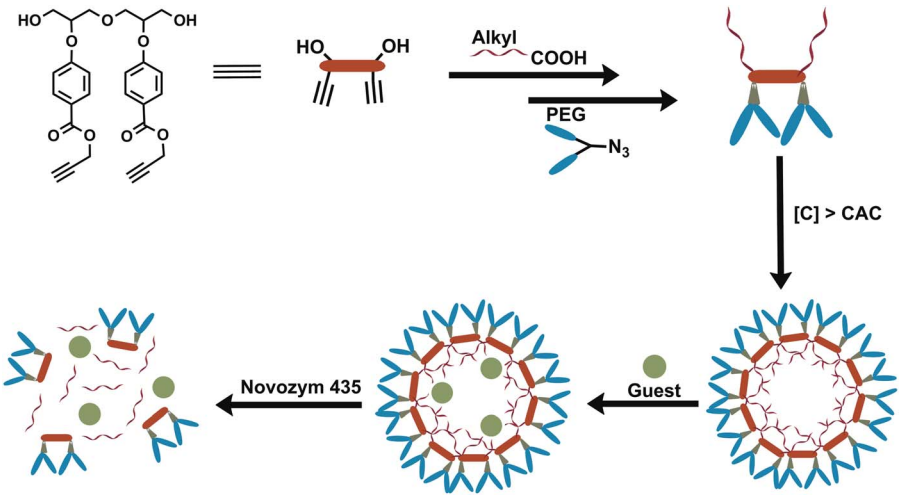

Fig. 1 Representation of synthesis, self-assembly of the amphiphiles, guest encapsulation and its release under hydrolytic conditions using the enzyme Novozym 435.

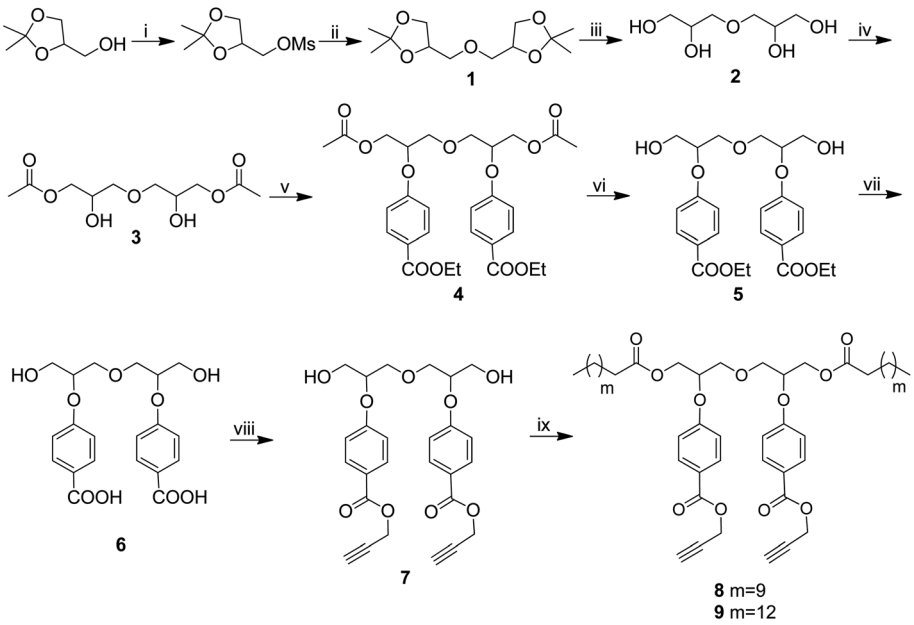

Scheme 1 Synthesis of hydrophobic moiety: (i) MsCl, triethyl amine, DCM, 0–25 °C, 2 h; (ii) solketal, KOH, TBAB, toluene, 70 °C, 40 h; (iii) Dowex 50wx8, methanol, 50 °C, 12 h; (iv) vinyl acetate, Novozym 435, THF, 30 °C, 12 h; (v) ethyl *p*-hydroxybenzoate, DIAD, triphenylphosphine, THF, 25 °C, 15 h; (vi) K_2CO_3, ethanol, 25 °C, 12 h; (vii) KOH, ethanol, 80 °C, 12 h; (viii) K_2CO_3, propargyl bromide, DMF, 50 °C, 12 h; (ix) *n*-alkyl carboxylic acid, EDC·HCl, DMAP, DCM, 25 °C, 12 h.

bromide to obtain the compound **7**. Incorporating lipophilic long chain aliphatic acid (C-12/C-15) *via* the primary hydroxyl groups of **7** followed by coupling of hydrophilic mPEG azide (M_n: 350/550 g mol^{-1}) *via* copper catalyzed Click reaction led to the synthesis of the amphiphilic architectures **15–18** (Schemes 1–3). The physicochemical and supramolecular organization behavior of the resulting amphiphiles were studied using various spectroscopic and analytical techniques, *i.e.*, NMR, IR, UV-vis, fluorescence spectroscopy, gel permeation chromatography (GPC), and DLS.

3.1. Synthesis and characterization

An A_2B_2 monomer (**7**) bearing a dialkyne system was first synthesized from diglycerol (**2**) by the procedure outlined in Scheme 1.

Diglycerol in turn was synthesized from the coupling of commercially available solketal with its mesyl derivative to yield protected diglycerol (3,3′-oxybis(propane-1,2-diol)) (**1**). The compound **1** was then hydrolyzed using cationic Dowex to yield diglycerol (**2**). The primary hydroxyls of diglycerol were chemoselectively acylated using vinyl acetate in the presence of immobilized *Candida antarctica* lipase (Novozym 435) following the literature procedure[31] to give compound **3**. The unreacted secondary hydroxyl groups of the compound **3** were then coupled with ethyl *p*-hydroxybenzoate *via* Mitsunobu reaction to yield compound **4**, on treatment with ethanolic potassium carbonate compound **4** undergoes chemo-selective aliphatic acid ester hydrolysis to yield compound **5**. The dihydroxy compound so obtained was purified by column chromatography and then subjected for further hydrolysis using ethanol and potassium hydroxide yielding diaryloxydiglycerol (**6**), which was found to be sufficiently pure and suitable to act as a precursor of central core (**7**) for the synthesis of amphiphiles around it. Treatment of diaryloxydiglycerol (**6**) with propargyl bromide in the presence of potassium carbonate yield dipropargyl derivative **7**, which was coupled with dodecanoic/pentadecanoic acid using *N*-(3-dimethylaminopropyl)-*N*-ethylcarbodiimide hydrochloride (EDC·HCl) to yield compounds **8** and **9**, respectively.

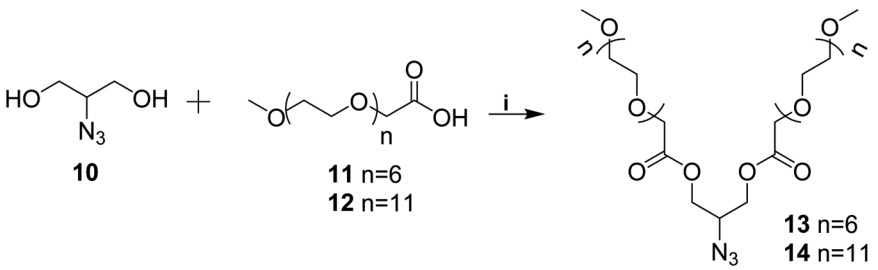

Scheme 2 Synthesis of hydrophilic moiety: (i) EDC·HCl, DMAP, DCM, 35 °C, 12 h.

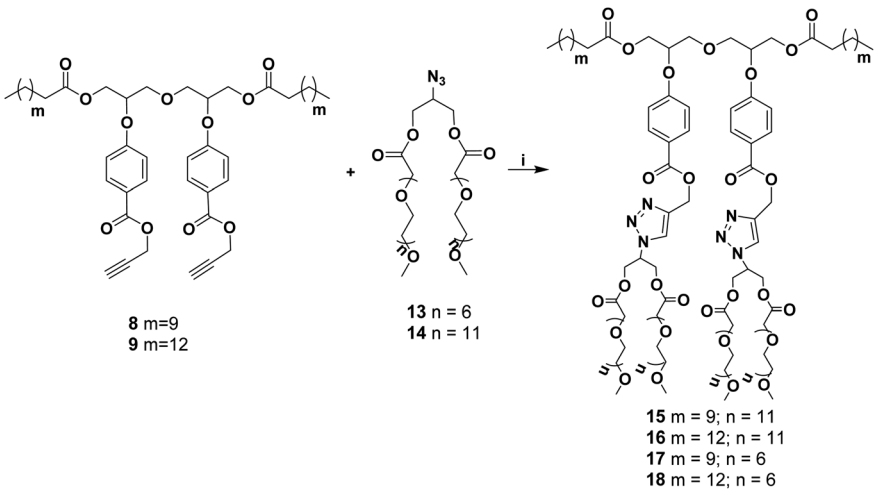

Scheme 3 Synthesis of amphiphiles: (i) $[Cu(PPh_3)_3]Br$, DIPEA, DMF, 60 °C, 24 h.

Azido-glycerol (**10**) and mPEG acids (**11**/**12**) were coupled using EDC·HCl and DMAP (Scheme 2) to yield mPEG based hydrophilic moieties (**13**/**14**). mPEG acids (**11**/**12**) and azido-glycerol (**10**) in turn were synthesized following the earlier reported procedure by our group[31,32] Azide functionality onto the hydrophilic moiety (**13**/**14**) facilitated its coupling with the compound **8**/**9** simply by Click reaction (Scheme 3) to yield amphiphiles **15–18** in quantitative yield.

3.2. Physicochemical characterization and self-assembly study of amphiphiles in aqueous medium

All of the synthesized amphiphiles (**15–18**) showed supramolecular aggregation behavior in aqueous medium. The critical aggregation concentration (CAC) measurement of the resulting micelles was performed by fluorescence spectrophotometer. DLS measurements were used for determining the particle size. To have an idea about the morphology of the nanocarriers transmission electron microscopy (TEM) micrograph was also recorded.

3.2.1. Critical aggregation concentration measurement using fluorescence spectroscopy. The CAC of the synthesized amphiphiles **15–18** was measured by fluorescence spectrophotometer, using Nile red as a fluorescent probe.[33] Nile red has very poor aqueous solubility and it exhibits prominent solvatochromic effect, it shows strong fluorescence in hydrophobic environment, *i.e.*, on encapsulation by supramolecular architectures.[34] Furthermore, it was observed that at a specific amphiphile concentration in aqueous medium, a noticeable increment in the fluorescent intensity of the dye was observed, this is referred to as the minimum concentration at which the molecules form aggregates (CAC). The plot of fluorescence intensity of encapsulated Nile red *versus* log[amphiphile concentration] (Fig. S13, ESI†) provides the CAC value of the amphiphiles. The CAC value of the synthesized amphiphiles lies in the range of 3.994×10^{-6} to 1.140×10^{-4} M and it was observed that by varying the mPEG from M_n: 350 to 550 led to the lowering of CAC *i.e.* the amphiphiles **15** and **16** consisting of mPEG 550 hydrophilic moiety and C-12/C-15 alkyl chain have lower CAC values as compared to their corresponding analogues **17** and **18** containing relatively smaller mPEG (M_n: 350) units (Table 1). The HLB value of all the amphiphiles was evaluated by the Griffin equation (Table 1). Furthermore, a comparison of these diaryloxydiglycerol based amphiphiles (**15** and **16**) having lower CAC with the previously reported triaryloxytriglyceryl analogue **19**/**20** synthesized by earlier reported method[35] shows that on moving from triaryloxytriglycerol

Table 1 Physico-chemical data of amphiphiles

	DLS size (nm)			
Amphiphile	Intensity	Volume	CAC (M)	HLB = 20 × M_h[a]/MW[b]
C-12/DG/mPEG-550 (**15**)	10.11	10.11	3.944×10^{-6}	15.51
C-15/DG/mPEG-550 (**16**)	10.12	10.53	3.175×10^{-6}	15.43
C-12/DG/mPEG-350 (**17**)	8.91	8.95	1.14×10^{-4}	15.68
C-15/DG/mPEG-350 (**18**)	10.13	11.65	7.14×10^{-5}	15.46
C-15/TG/mPEG-550 (**19**)	10.15	—	6.196×10^{-5}	15.04
C-15/TG/mPEG-350 (**20**)	10.83	—	5.208×10^{-5}	12.23

[a] Molecular weight of hydrophilic part. [b] Molecular weight of amphiphiles determined by GPC.

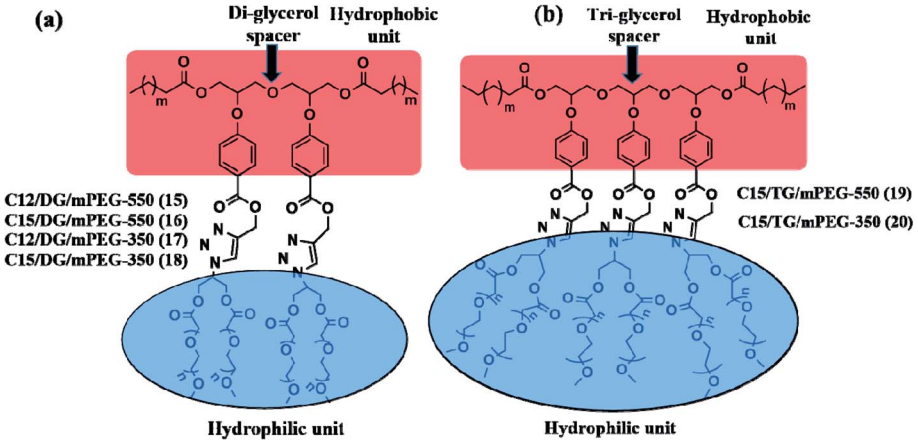

Fig. 2 Structure of (a) diaryloxydiglycerol based and (b)[35] triaryloxytriglycerol based amphiphilic architectures.

Table 2 Transport behavior of the amphiphiles for Nile red and nimodipine

	Transport efficiency (mg g^{-1})		Transport capacity (mmol mol^{-1})		Encapsulation efficiency (%)	
Amphiphile	Nile red	Nimodipine	Nile red	Nimodipine	Nile red	Nimodipine
15	1.55	22.60	16.80	186.14	6.46	14.13
16	1.99	23.00	21.50	188.96	8.28	14.38
17	0.38	15.67	02.85	89.14	1.58	9.79
18	0.42	17.37	03.17	100.24	1.75	10.85
19	3.38	39.00	51.60	440.21	8.47	24.38
20	1.57	37.46	18.07	344.70	3.90	23.41

spacer to diaryloxydiglycerol spacer reduces the CAC (Fig. 2 and Table 1) and this improvement in CAC may be because of proper structural balance of hydrophobic and hydrophilic segments.

3.2.2. Aggregation, particle size, and morphological study of amphiphiles using DLS and TEM. DLS was used to study the aggregation behavior and measure the hydrodynamic size of the particles formed in aqueous medium by the amphiphiles at a concentration of 5 mg mL^{-1} (Table 1). The particle size of the aggregates was found to be ranging from 7 to 9 nm (Fig. 3) for all of the four amphiphiles synthesized. Intensity and volume distribution plots of the amphiphiles are shown in Fig. 3. The size distribution profile was monomodal in volume and number, whereas it was bimodal in intensity. The two peaks present in the intensity distribution profile may be assigned to micelles and micellar aggregates, whereas a single peak in volume and number could be corresponding to micelles. It suggests that micellar aggregates are present in very small proportion, whereas micelles are the predominant species in the aqueous solution. To check the long-term stability, we recorded DLS at different time intervals over a period of nearly

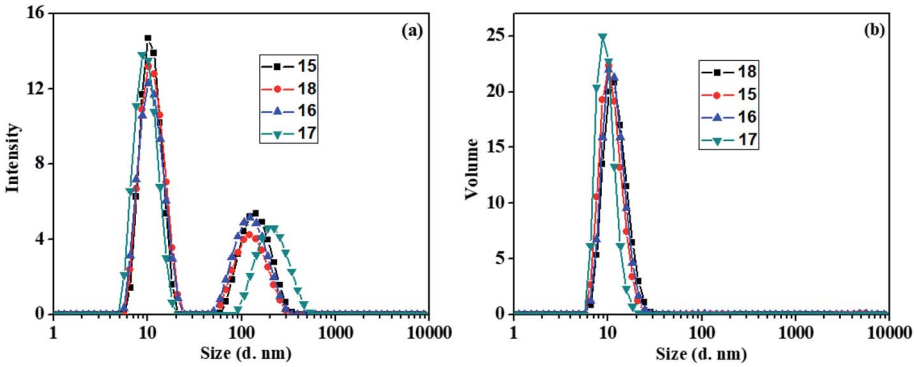

Fig. 3 DLS size distribution plots for the amphiphiles **15–18** in water (a) intensity distribution and (b) volume distribution.

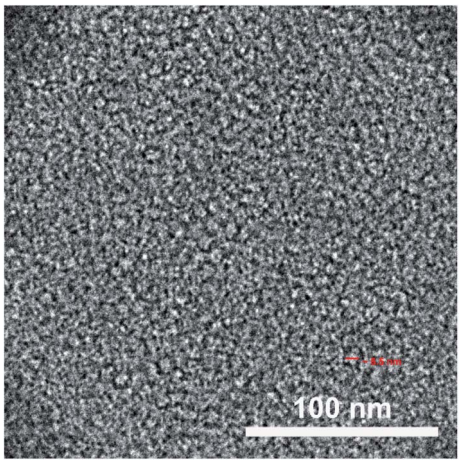

Fig. 4 TEM micrograph of amphiphile **16**.

two weeks and didn't observe any noticeable change in the light scattering data thus suggesting the nanoparticles to be stable enough. The formation of nano-sized aggregates of a size up to 200 nm is appropriate for biological applications as these can be used for prolonged delivery of therapeutic agents and enhanced drug uptake as compared to microparticles.[36] The TEM micrograph for amphiphile **16** (Fig. 4) shows micelles with a diameter of nearly 6 nm. These results are in good agreement with the DLS data, as the hydration shell does not contribute density in the visible assembly structure.

3.3. Cytotoxicity study

Cytotoxicity data is crucial for consideration of an amphiphile to be suitable for biomedical applications. The cytotoxicity study for the synthesized amphiphiles **15–18** was carried out by incubating the HeLa cells with amphiphiles at the concentration of 0.5, 0.1 and 0.05 mg mL^{-1} and analyzed by the cell viability measurement using the colorimetric CCK-8 assay (Fig. 5). The assay results revealed that all the synthesized amphiphiles are non-toxic up to a concentration of 0.1 mg mL^{-1}, though amphiphile **18** exhibits slight toxicity at 0.5 mg mL^{-1} (Fig. 5).

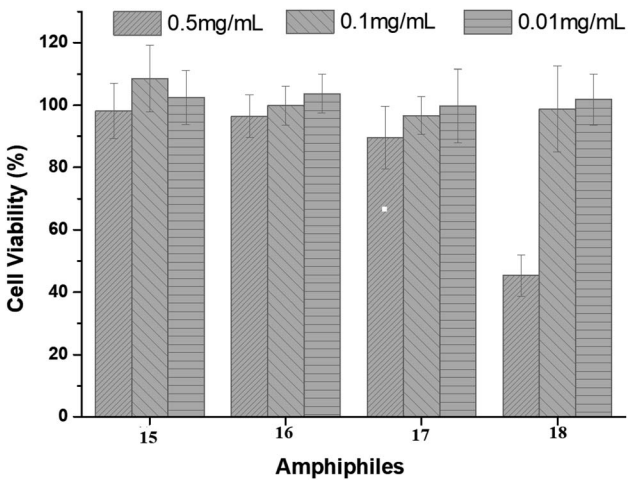

Fig. 5 Cytotoxicity profile of amphiphiles **15–18** after 24 h using HeLa cells. Each bar represents the mean value of three independent experiments ($n = 3$) and the standard deviation.

3.4. Transport studies

The significant importance of nanocarriers in the field of biomedicine such as drug delivery motivated us to carry out the encapsulation studies of the synthesized aqueous soluble amphiphiles **15–18** using a model hydrophobic drug 'nimodipine', a 1,4-dihydropyridine derivative and a well-known calcium channel blocker. Also, it helps in maintaining the cerebral blood flow in humans and animals.[37] In addition, a model hydrophobic dye Nile red was used for the evaluation of the transport potential of the resulting amphiphilic systems. Nile red encapsulation furnishes useful information about the site of encapsulation in nanocarriers as it exhibits a strong emission in a lipophilic environment.[34] Nile red and nimodipine encapsulation in the amphiphilic systems was accomplished by either the film method[34] or solid dispersion method.[38] An aqueous amphiphilic solution (5 mg mL^{-1}) was used to encapsulate 0.12/0.5 mg of Nile red/nimodipine. The quantification of encapsulated dye/drug was achieved by lyophilization of the encapsulated samples and measurement of their absorbance spectra after re-dissolving in a known quantity of methanol (for Nile red) or ethanol (for nimodipine). The transport efficiency (Fig. S14a, ESI†), transport capacity (Fig. S14b, ESI†) and encapsulation efficiency of the synthesized amphiphiles for the encapsulated Nile red/nimodipine (Table 2) were calculated by using the Beer–Lambert's law and the molar extinction coefficient (ε) of 45 000 M^{-1} cm^{-1} at 552 nm for Nile red in methanol or 7200 M^{-1} cm^{-1} at 356 nm for nimodipine in ethanol.[39]

Comparison of the transport potential *i.e.* the transport efficiency, transport capacity and encapsulation efficiency of the amphiphiles **15–18** for nimodipine and Nile red reveals that longer (C-15) alkyl chain containing amphiphiles **16** and **18** are better nano-transporters as compared to their analogues **15** and **17** with shorter (C-12) alkyl moiety, thus suggesting hydrophobicity to play a key role in enhancing the transport potential. Similarly, while comparing the effect of PEG size, it was observed that the amphiphiles **15** and **16** with larger hydrophilic PEG (M_n: 550) moiety have improved transport potential as compared to those with smaller PEG (M_n: 350) *i.e.* amphiphiles **17** and **18**. Larger PEG improves the CAC for compounds **15** and **16** ($\sim 10^{-6}$ M) and the micelles formed are more stable and have better encapsulation efficiency for Nile red and nimodipine, but the amphiphiles **17** and **18** are not so efficient to encapsulate in particular the highly hydrophobic dye Nile red due to their lesser hydrophilic content and hence the difference in encapsulation efficiency for the mentioned guests *i.e.* dye and drug nimodipine is large. However, these amphiphiles reported here constituted from diaryloxydiglycerol core have inferior transport potential as compared to the amphiphiles **19** and **20** consisting of triaryloxytriglycerol core reported earlier by our group (Fig. 2).[35]

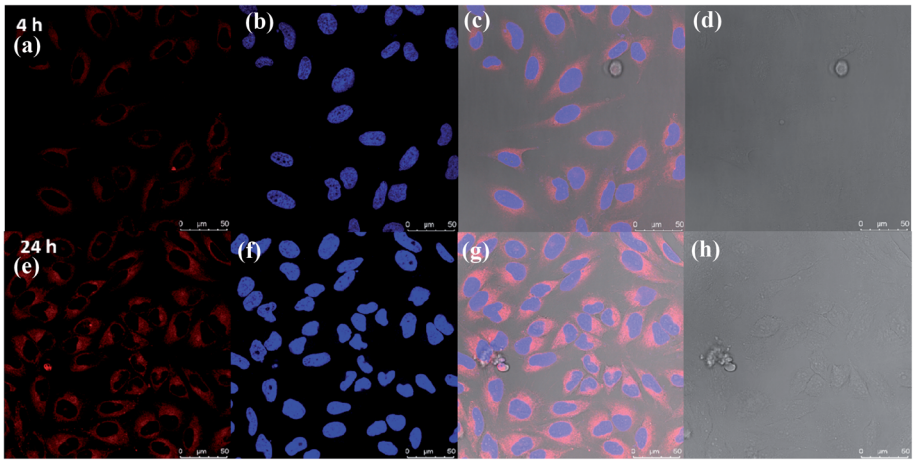

Fig. 6 Confocal laser scanning fluorescence microscopy images from HeLa cells after 4 h (a–d) and 24 h (e–h) incubation of Nile red encapsulated in amphiphile **16**. In the images, Nile red is shown in red color and blue color indicates the nucleus stained with Hoechst 33342. The scale bar equals 50 μm.

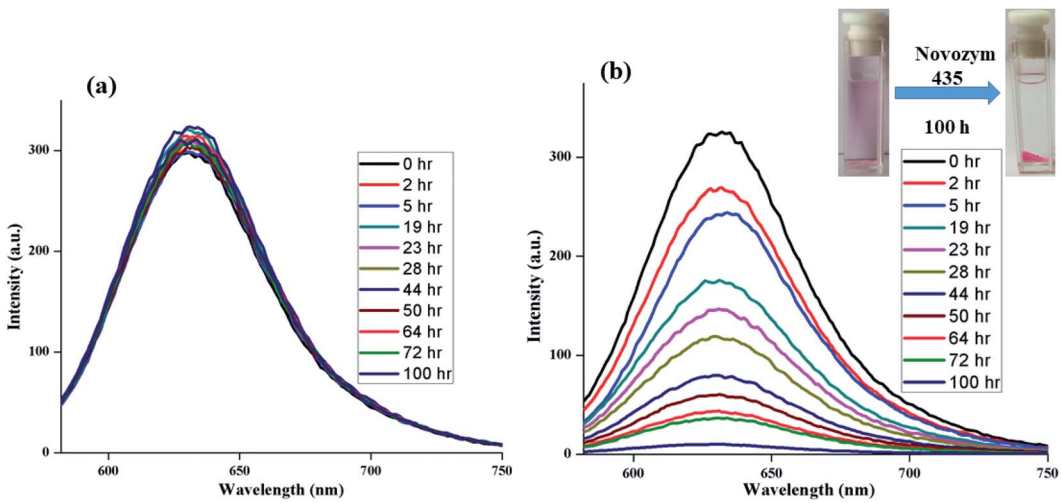

Fig. 7 Study of release of encapsulated Nile red from nanocarrier **16** under physiological conditions by measuring the intensity of emission of encapsulated dye at 37 °C (a) in the absence of enzyme; and (b) in the presence of enzyme.

3.5. Cellular uptake study

Because of the observance of the highest encapsulation of Nile red by amphiphile **16**, this was shortlisted for further studying the cellular uptake potential by confocal laser scanning microscopy (cLSM) using HeLa cells. The cLSM images (Fig. 6) show that after 4 h of incubation, a strong signal is seen inside the cell's cytosol. After 24 h an increase of the intensity of Nile red was seen, which indicate that Nile red is accumulating in cells with time. These results indicate that the amphiphile is well suited as a drug delivery system.

3.6. Enzyme-triggered release of encapsulated guest

Besides encapsulation and cellular uptake, triggering the release of guest in a controlled manner is of paramount importance. Since the amphiphiles contain ester functionality, we employed a general de-esterification method using Novozym 435 to investigate the time-dependent release of the encapsulated guest from the core of nanocarriers by measuring fluorescence at regular intervals. It was observed that the complete release of encapsulated dye takes place within 100 h, however no noticeable release of encapsulated dye was observed in the absence of the enzyme (Fig. 7).

4. Conclusions

A new series of diaryloxydiglycerol-based amphiphiles have been designed and synthesized using a biocompatible starting material like glycerol, *p*-hydroxybenzoic acid, and mPEG, these self-assemble into supramolecular architectures. All the synthesized amphiphiles were completely characterized by IR, ^{1}H and ^{13}C-NMR spectra, and GPC techniques. Investigation of the self-assembly behavior of the synthesized amphiphiles was carried out using DLS, which confirmed that amphiphiles form

small-sized aggregates with hydrodynamic diameter in the 8–11 nm range and form aggregates at low concentration of the order of 10^{-4} to 10^{-6} M. The TEM study of amphiphile also confirmed the formation of aggregates in nm range. For evaluating the encapsulation potential, Nile red was used as a model dye and nimodipine as a model drug. Among the amphiphiles **15–18**, compound **16** having C-15 alkyl chain and mPEG-550 moiety has the highest encapsulation potential and shows an efficient dye release from the hydrophobic core of the amphiphile on exposure to enzyme. On comparison, the transport potential of the amphiphiles synthesized herein from diaryloxydiglycerol core were found to be inferior as compared to the one synthesized earlier using triaryloxytriglycerol core. Though an opposite trend was observed for CAC value *i.e.* the amphiphiles constructed from diaryloxydiglycerol core have lower CAC value as compared to triaryloxytriglycerol core. Cytotoxicity profile was also obtained by using HeLa cancer cell lines, which showed that the synthesized amphiphiles are relevant as drug delivery system. Furthermore, the stimuli responsive release of the encapsulated guest from the hydrophobic core of amphiphilic aggregates using immobilized *Candida antarctica* lipase (Novozym 435) at 37 °C was also investigated. The present data testify the potential of these newer amphiphiles for the design and development of efficient nanocarriers for biomedical applications.

Conflicts of interest

There are no conflicts to declare.

Acknowledgements

The authors gratefully acknowledge the financial support from DST, Government of India, and DFG, Germany for supporting a collaboration research project (Grant No. INT/FRG/DFG/P-03/2017). The authors would like to thank Elisa Quaas for performing cell viability experiments. The authors would also like to acknowledge CSIR-UGC, New Delhi for providing fellowships to Parmanand, Aarti and Ayushi Mittal and the assistance of the Core Facility BioSupraMol supported by the DFG.

References

1 C. Branden and J. Tooze, *Introduction to protein structure*, Garland Publishing Inc., New York, 2nd edn, 1999.
2 V. Percec, A. E. Dulcey, V. S. K. Balagurusamy, Y. Miura, J. Smidrkal, M. Peterca, S. Nummelin, U. Edlund, S. D. Hudson, P. A. Heiney, H. Duan, S. N. Magonov and S. A. Vinogradov, *Nature*, 2004, **430**, 764–768.
3 M. A. Alam, Y. S. Kim, S. Ogawa, A. Tsuda, N. Ishii and T. Aida, *Angew. Chem., Int. Ed.*, 2008, **47**, 2070–2073.
4 J. D. Badjić, A. Nelson, S. J. Cantrill, W. B. Turnbull and J. F. Stoddart, *Acc. Chem. Res.*, 2005, **38**, 723–732.
5 M. Lee, B. K. Cho and W. C. Zin, *Chem. Rev.*, 2001, **101**, 3869–3892.
6 J. A. A. W. Elemans, A. E. Rowan and R. J. M. Nolte, *J. Mater. Chem.*, 2003, **13**, 2661–2670.
7 S. I. Stupp and L. C. Palmer, *Chem. Mater.*, 2014, **26**, 507–518.
8 J. Shi, Z. Xiao, N. Kamaly and O. C. Farokhzad, *Acc. Chem. Res.*, 2011, **44**, 1123–1134.
9 B. Y. Wang, H. Xu and X. Zhang, *Adv. Mater.*, 2009, **21**, 2849–2864.
10 D. A. LaVan, T. McGuire and R. Langer, *Nat. Biotechnol.*, 2003, **21**, 1184–1191.
11 H. Otsuka, Y. Nagasaki and K. Kataoka, *Adv. Drug Delivery Rev.*, 2003, **55**, 403–419.
12 R. Haag and F. Kratz, *Angew. Chem., Int. Ed.*, 2006, **45**, 1198–1215.
13 S. Gupta, R. Tyagi, V. S. Parmar, S. K. Sharma and R. Haag, *Polymer*, 2012, **53**, 3053–3078.
14 R. Duncan, *Nat. Rev. Drug Discovery*, 2003, **2**, 347–360.
15 R. Satchi-Fainaro, R. Duncan and C. M. Barnes, *Adv. Polym. Sci.*, 2006, **193**, 1–65.
16 S. Prasad, K. Achazi, B. Schade, R. Haag and S. K. Sharma, *Eur. Polym. J.*, 2018, **109**, 506–522.
17 A. Sharma and A. Kakkar, *Molecules*, 2015, **20**, 16987–17015.
18 J. Khandare, M. Calderón, N. M. Dagia and R. Haag, *Chem. Soc. Rev.*, 2012, **41**, 2824–2848.
19 R. A. Shirwaiker, M. F. Purser and R. A. Wysk, in *Rapid Prototyping of Biomaterials: Principles and Applications*, ed. R. Narayan, Woodhead Publishing, 2014, ch. 6, pp. 176–200.
20 F. S. T. Mirakabad, K. Nejati-Koshki, A. Akbarzadeh, M. R. Yamchi, M. Milani, N. Zarghami, V. Zeighamian, A. Rahimzadeh, S. Alimohammadi, Y. Hanifehpour and S. W. Joo, *Asian Pac. J. Cancer Prev.*, 2014, **15**(2), 517–535.
21 H. Lv, S. Zhang, B. Wang, S. Cui and J. Yan, *J. Controlled Release*, 2006, **114**, 100–109.
22 R. S. G. Krishnan, S. Thennarasu and A. B. Mandal, *J. Phys. Chem. B*, 2004, **108**, 8806–8816.
23 B. Trappmann, K. Ludwig, M. R. Radowski, A. Shukla, A. Mohr, H. Rehage, C. Böttcher and R. Haag, *J. Am. Chem. Soc.*, 2010, **132**, 11119–11124.
24 K. Urata, *Eur. J. Lipid Sci. Technol.*, 2003, **105**, 542–556.
25 M. O. Sonnati, S. Amigoni, E. P. Taffin de Givenchy, T. Darmanin, O. Chouletb and F. Guittard, *Green Chem.*, 2013, **15**, 283–306.
26 H. Baumann, M. Bühler, H. Fochem, F. Hirsinger, H. Zoebelein and J. Falbe, *Angew. Chem., Int. Ed. Engl.*, 1988, **27**, 41–62.
27 A. K. Singh, R. Nguyen, N. Galy, R. Haag, S. K. Sharma and C. Len, *Molecules*, 2016, **21**, 1038–1049.
28 P. Cintas, S. Tagliapietra, E. C. Gaudino, G. Palmisano and G. Cravotto, *Green Chem.*, 2014, **16**, 1056–1065.
29 B. Parshad, P. Yadav, Y. Kerkhoff, A. Mittal, K. Achazi, R. Haag and S. K. Sharma, *New J. Chem.*, 2019, **43**, 11984–11993.
30 B. Parshad, M. Kumari, K. Achazi, C. Böttcher, R. Haag and S. K. Sharma, *Polymers*, 2016, **8**, 311–325.
31 S. Gupta, B. Schade, S. Kumar, C. Böttcher, S. K. Sharma and R. Haag, *Small*, 2013, **9**, 894–904.
32 M. Kumari, A. K. Singh, S. Kumar, S. Gupta, K. Achazi, R. Haag and S. K. Sharma, *Polym. Adv. Technol.*, 2014, **25**, 1208–1215.

33 K. Nagy, S. Göktürk and L. Biczók, *J. Phys. Chem. A*, 2003, **107**, 8784–8790.
34 E. Fleige, B. Ziem, M. Grabolle, R. Haag and U. Resch-Genger, *Macromolecules*, 2012, **45**, 9452–9459.
35 A. Mittal, A. K. Singh, A. Kumar, Parmanand, K. Achazi, R. Haag and S. K. Sharma, *Polym. Adv. Technol.*, 2020, **31**, 1208–1217.
36 R. Singh and J. W. Lillard Jr, *Exp. Mol. Pathol.*, 2009, **86**, 215–223.
37 M. S. Langley and E. M. Sorkin, *Drugs*, 1989, **37**, 669–699.
38 V. Kumar, B. Gupta, G. Kumar, M. K. Pandey, E. Aiazian, V. S. Parmar, J. Kumar and A. C. Watterson, *J. Macromol. Sci., Part A: Pure Appl. Chem.*, 2010, **47**, 1154–1160.
39 R. P. Haugland, *Handbook of Fluorescent Probes and Research Chemicals*, Molecular Probes Inc., Eugene, OR, USA, 6th edn, 1996.